www.springer.com/41230
https://doi.org/10.1007/s41230-022-1191-2

Research & Development
Vol. 19 No. 5 September 2022
CHINA FOUNDRY

# Effect of La addition on semi-solid microstructure evolution of Mg-7Zn magnesium alloy

**Zhan-yu Zhang, *Xiao-feng Huang, Fan Yang, Sheng Zhang, and Jiao-li Fu**

*State Key Laboratory of Advanced Processing and Recycling of Nonferrous Metals, Lanzhou University of Technology, Lanzhou 730050, China*

**Abstract:** Semi-solid billets of Mg-7Zn and Mg-7Zn-0.3La alloys were prepared by semi-solid isothermal heat treatment. The effects of the La element on the as-cast and semi-solid microstructures of Mg-7Zn alloy were investigated. Meanwhile, the effects of isothermal temperature and holding time on the evolution of the semi-solid microstructure of Mg-7Zn-0.3La alloy were also studied. Results indicate that the addition of a small amount of La can significantly refine the as-cast and semi-solid microstructure. During the semi-solid thermal transformation, the size and shape factor of solid particles decrease at first and then increase with the increase of isothermal temperature and holding time. The semi-solid microstructure of Mg-7Zn-0.3La alloy obtained by holding at 605 °C for 30 min is the optimal. The average size of solid particles, shape factor, and solid fraction are 42 μm, 1.45 and 61.8%, respectively. At the same time, a comparative study on the coarsening process of particles in the semi-solid billets of Mg-7Zn and Mg-7Zn-0.3La alloys reveals that the addition of La effectively decreases the coarsening rate of solid particles and restricts the growth of solid particles.

**Keywords:** magnesium alloy; La element; semi-solid microstructure evolution; coarsening rate constant

**CLC numbers:** TG146.22 **Document code:** A **Article ID:** 1672-6421(2022)05-403-08

## 1 Introduction

Semi-solid metal (SSM) processing is one of the irreplaceable forming methods, as it combines the advantages of both forging and liquid metal forming. Compared with forging, SSM processing can be used to produce products with complex shapes. Simultaneously, it can avoid defects such as pores, shrinkage and porosity caused by liquid metal forming. Therefore, the workpiece produced by SSM processing has a compact structure, and the mechanical properties of workpieces can be further improved by heat treatment [1]. At the same time, it has been reported that SSM processing is beneficial to the preparation of high-performance magnesium matrix composites [2-3]. Therefore, it is of great significance to study the SSM processing technology of magnesium alloys for improving the application of magnesium alloys. The preparation of a semi-solid slurry or billet meeting the requirements of SSM processing is the key to SSM processing [4]. There are over 20 kinds of techniques to prepare semi-solid billets or slurries, such as magnetohydrodynamic stirring (MHD), recrystallization and partial melting (RAP), strain-induced melt activated (SIMA), and semi-solid isothermal heat treatment (SSIT), etc [5-7]. The SIMA process mainly includes two steps: deformation of as-cast billets and subsequent partial remelting. The principle of the MHD process is to obtain non-dendritic structures by stirring the alloy melt. These techniques will introduce extra costs. SSIT can complete the preparation of semi-solid billets during remelting without any special procedures. It shows more significant commercial advantages and is widely used [8-9].

The key to employing the advantage of SSM processing is to find alloys with ideal semi-solid microstructure that meet the requirements of SSM processing and have remarkable heat treatment strengthening. The most effective way to improve the structure and properties is achieved by alloying with a second constituent [10]. Rare earth (RE) elements are often used to modify magnesium alloys [11-13]. Previous studies have found that adding an appropriate amount of La into magnesium alloys can not only refine the grain size but also improve the mechanical properties of Mg-Al-Zn series alloys after heat treatment [14-15]. Du et al. [16] found that microalloying with La significantly refined the grain size and enhanced the ductility of Mg-6Zn alloy. Nami et al. [17] found that the solid-liquid interfacial energy was reduced caused by the addition of RE elements in AZ91 alloy.

***Xiao-feng Huang**

Male, born in 1971, Ph. D., Associate professor. His research interests mainly focus on magnesium alloys and semi-solid forming. He has published over 80 papers.

E-mail: huangxf_lut@163.com

**Received: 2021-11-01; Accepted: 2022-04-11**

As a result, the coarsening rate of solid particles decreases. In order to design a new magnesium alloy suitable for SSM processing, some scholars studied the influence of different alloying elements on the magnesium alloy during the SSIT process. They found that for the preparation of semi-solid billets by SSIT, the alloys should have a wide semi-solid temperature range [18]. The semi-solid temperature range of Mg-Zn alloy is wide [19-20]. A study of binary Mg-Zn alloys shows that when the Zn content is 7wt.%, the solid particles obtained by SSIT are smaller and rounder than other Mg-Zn alloys [21]. At the same time, Mg-Zn alloys can be heat treated to give superior mechanical properties [22-23].

In this work, La element was added to further improve the quality of semi-solid billets of Mg-7Zn alloy, and the effect of La element on the semi-solid microstructure of Mg-Zn series magnesium alloys was investigated. Accordingly, the semi-solid microstructure evolution of Mg-7Zn-0.3La alloy during the SSIT process was studied, especially the effect of La element on the refinement of solid particles and the change of coarsening rate constant.

# 2 Experimental procedure

Castings with nominal compositions of Mg-7Zn (all the compositions are given in wt.% unless otherwise noted) and Mg-7Zn-0.3La alloys were prepared with pure Mg (99.99%), commercial high purity Zn ingot (99.9%), and Mg-30%La master alloy by melting in a pit-type SG2-7.5 kW electric resistance furnace. After the Mg ingot was completely melted, Zn ingot and Mg-30%La master alloy were added into the melt at 680 °C. The temperature of the melt was raised to 750 °C and then cooled to 730 °C. Subsequently, 0.2% $C_2Cl_6$ (ratio to the total mass of raw materials) was added to the melt by mechanical stirring for 3 min to refine and remove scum. Meanwhile, RJ-2 covering flux and an atmosphere of Ar were used to shield the melt from oxidation and burning in the whole process of melting. Finally, at 710 °C, the melt was poured into a permanent steel mold pre-heated to 150 °C. The obtained castings with the dimension of $\Phi$18 mm×110 mm were cut into specimens with the size of $\Phi$18 mm×15 mm.

The SSIT process was performed in a box-type resistance furnace. After reaching the experimental temperatures (575, 585, 595, 605, 615, and 625 °C), the samples were held for different time durations (5, 10, 20, 30, 40, 50, 60, 90, and 120 min), and then taken out for water quenching quickly. All as-cast and semi-solid specimens were etched by picric acid reagent (3 g picric acid, 20 mL acetic acid, 20 mL distilled water and 50 mL alcohol) and 8% $HNO_3$ water solution in turn. An optical microscope (OM) and a JSM-6700F scanning electron microscope (SEM) equipped with an energy dispersive spectrometer (EDS) were adopted to characterize microstructures and chemical compositions of the as-cast specimens and semi-solid samples. In this work, the average particle size ($d_0$) and shape factor ($f_0$) of semi-solid microstructure were calculated by the Image-Pro Plus software according to the following equations [24]:

$$d_0 = \left[ \sum 2(A_0/\pi)^{\frac{1}{2}} \right] / n \quad (1)$$

$$f_0 = (\sum P_0^2 / 4\pi A_0) / n \quad (2)$$

where $A_0$ is the area of the solid particle, $P_0$ is the perimeter of each solid particle, and $n$ is the number of solid particles. The closer the $f_0$ is to 1, the more rounded the solid grains.

# 3 Results and discussion

## 3.1 As-cast microstructure

OM and SEM micrographs of the experimental alloys are shown in Fig. 1. Compared with microstructures of La-free alloy, the microstructures adding La element show noticeable changes. The average grain size of the alloy decreases from 98 μm to 61 μm with the addition of La element. The OM micrographs of as-cast Mg-7Zn alloy [Fig. 1(a)] and Mg-7Zn-0.3La alloy [Fig. 1(c)] show that eutectic phases are distributed within grains and along the grain boundaries. It can be clearly seen from Fig. 1(a) that the eutectic morphologies of Mg-7Zn alloy are mainly discontinuous island and in granular shape. However, the eutectic morphology of Mg-7Zn-0.3La alloy, compared with the La-free alloy, becomes more continuous as shown in Fig. 1(c). This phenomenon indicates that the addition of La is conducive to the formation of the continuous eutectic phase. SEM images of the experimental alloys were taken at a higher magnification, as shown in Figs. 1(b) and (d). The EDS point analyzed at several regions in each micrograph were conducted to identify the atomic percent of elements in different locations of the microstructure. The EDS results are shown in Table 1. As can be seen from Table 1, the content of La element is higher in continuous phases, which further indicates that the addition of La contributes to the formation of the continuous eutectic phase. The grain refinement of the Mg-7Zn-0.3La alloy is mainly due to the following two reasons: on the one hand, the addition of La can create concentration undercooling which suppresses the grain growth [16]. On the other hand, the continuous eutectic phase effectively inhibits grain growth during solidification, resulting in grain refinement [25].

## 3.2 Effect of La on semi-solid microstructure

Semi-solid microstructures of Mg-7Zn-$x$La ($x$=0, 0.3) alloys heat treated at 605 °C and held for 30 min are shown in Fig. 2. Compared with Mg-7Zn alloy [Fig. 2(a)], the solid particles of the semi-solid billet of the Mg-7Zn-0.3La alloy [Fig. 2(b)] have a smaller size, better roundness, and almost equal size in the whole zones. The average particle size of the Mg-7Zn-0.3La alloy is 42 μm, while that of the Mg-7Zn alloy is 75 μm. The main reason for this phenomenon is that the addition of La can effectively refine the grain size of the Mg-7Zn alloy and promote the formation of the continuous eutectic phase [8]. The eutectic phase melts firstly during the SSIT process. The island-like eutectic phase tends to form a small liquid pool inside the solid

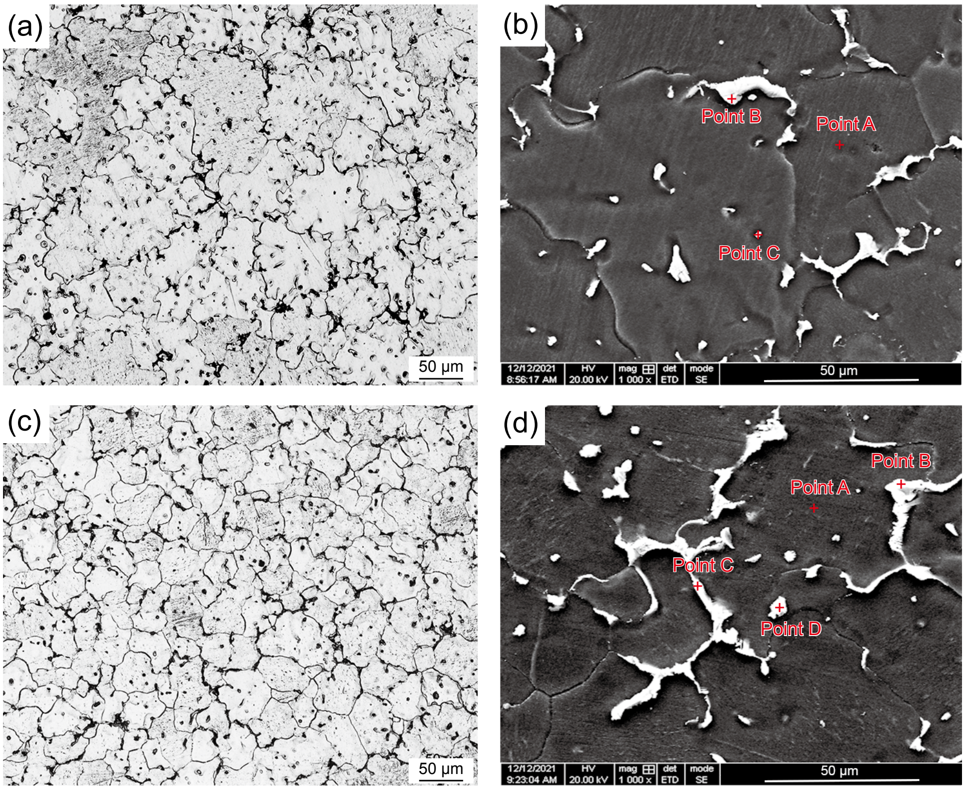


Fig. 1: OM (a, c) and SEM (b, d) microstructures of as-cast alloys: (a, b) Mg-7Zn alloy; (c, d) Mg-7Zn-0.3La alloy

Table 1: EDS analysis results of as-cast alloys

| Alloys | Points | Element contents (at.%) | | |
|---|---|---|---|---|
| | | Mg | Zn | La |
| Mg-7Zn | A | 98.6 | 1.4 | - |
| | B | 63.6 | 36.4 | - |
| | C | 74.5 | 25.5 | - |
| Mg-7Zn-0.3La | A | 98.9 | 1.1 | 0.0 |
| | B | 91.7 | 7.8 | 0.5 |
| | C | 72.4 | 27.3 | 0.3 |
| | D | 76.3 | 23.7 | 0.0 |

particles. Therefore, the continuous eutectic phase after melting can effectively promote the separation of solid particles, and then achieve smaller solid particles.

## 3.3 Semi-solid microstructural evolution

In this section, the effect of isothermal temperature and holding time on the average particle size, shape factor, and solid fraction were studied to determine the optimal process of SSIT for Mg-7Zn-0.3La alloy.

### 3.3.1 Effect of isothermal temperature on semi-solid microstructure

Figure 3 displays the optical micrographs of semi-solid microstructures of the Mg-7Zn-0.3La alloy treated at various temperatures for 30 min. Figure 4 shows the change of the average particle size, shape factor, and solid fraction of the

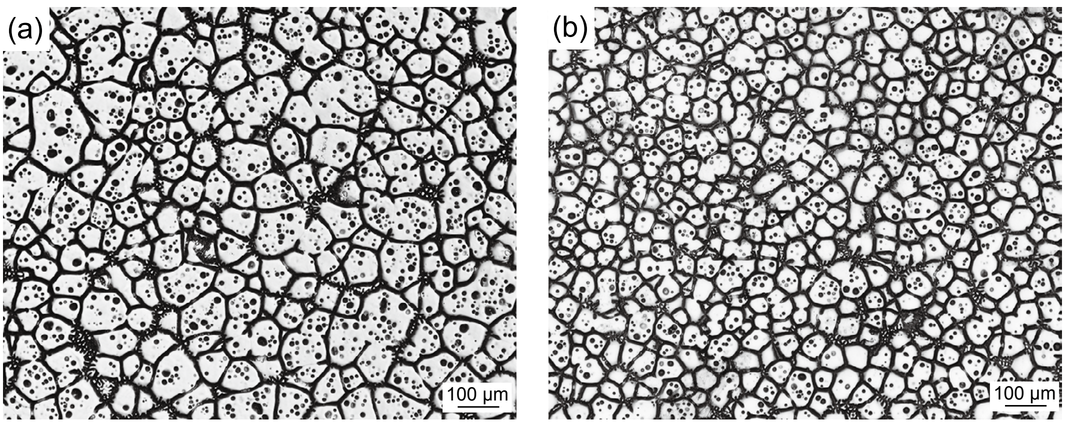


Fig. 2: Semi-solid microstructures of Mg-7Zn (a) and Mg-7Zn-0.3La (b) alloys heat treated at 605 °C for 30 min

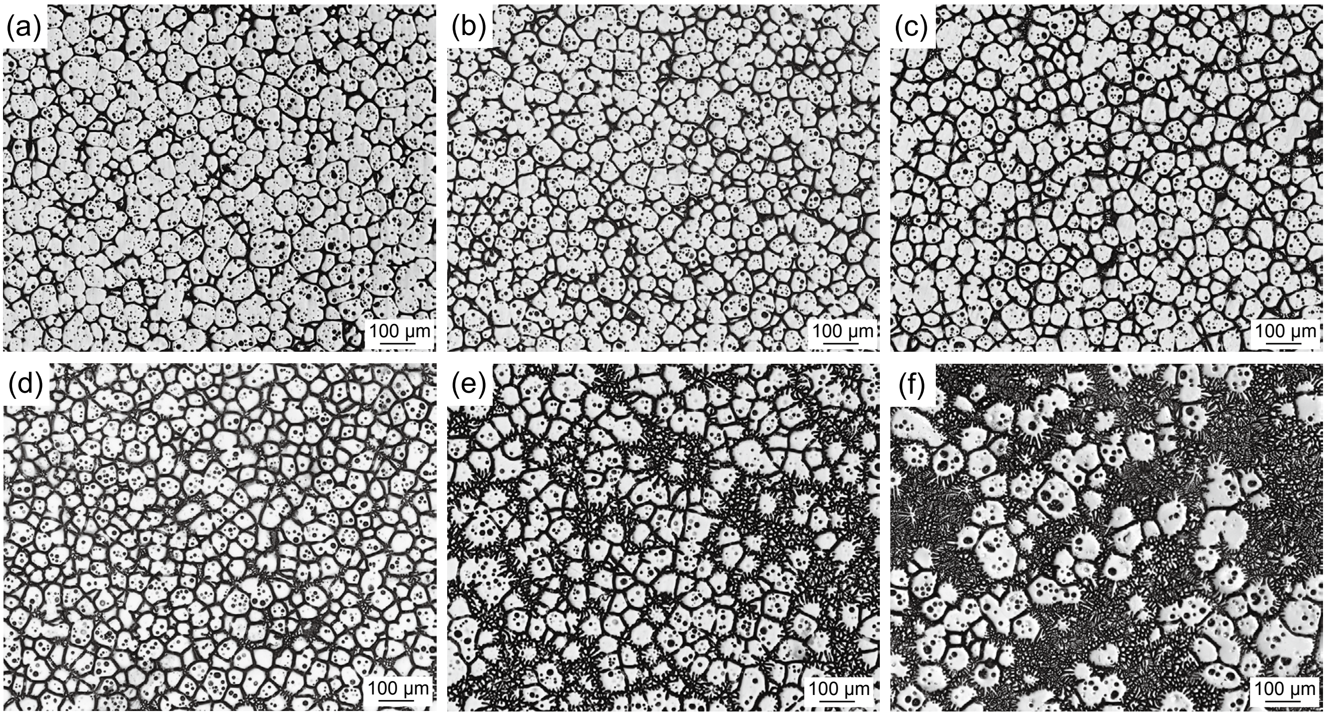


**Fig. 3: Optical microstructures of semi-solid Mg-7Zn-0.3La alloy treated for 30 min at different temperatures: (a) 575 °C; (b) 585 °C; (c) 595 °C; (d) 605 °C; (e) 615 °C; (f) 625 °C**

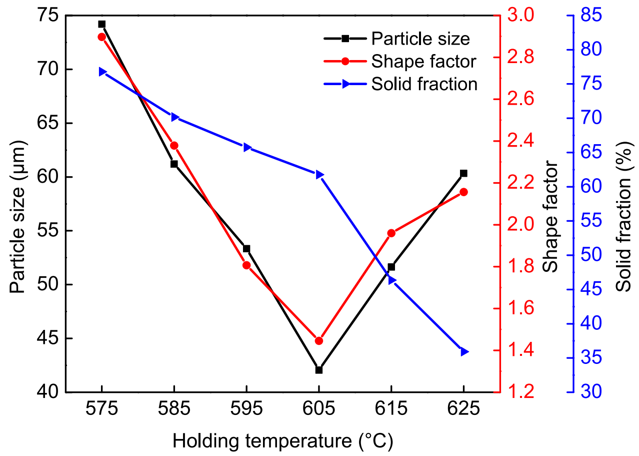


**Fig. 4: Variation of average particle size, shape factor, and solid fraction with isothermal temperature for semi-solid Mg-7Zn-0.3La alloy**

alloy. As seen from Fig. 3, the semi-solid microstructure of the alloy consists of solid particles and liquid phase. Meanwhile, with the increase of isothermal temperature, the liquid fraction gradually increases. It can be seen from Fig. 3(a) that after holding at 575 °C for 30 min, the solid particles cannot be separated at a lower temperature, resulting in the large size and irregular shape of the solid particles. As observed in Figs. 3(b) and (c), with the temperature increasing to 585 °C and 595 °C, solid particles are clearly separated and fine particles form gradually. When the isothermal temperature is 605 °C, as observed in Fig. 3(d) and Fig. 4, the size and shape factor of solid particles of the alloy are the smallest. The solid particles become more spherical. The spherification stage is a significant stage of semi-solid microstructure evolution in the SSIT process, which makes the solid particles with irregular shapes tend to be round. The spheroidization of solid particles relates to the curvature of the particle interface, which determines the change of the equilibrium melting point ($\Delta T_r$) of the alloy. The relationship between the equilibrium melting point of the alloy and the curvature of the particle interface can be expressed as [26]:

$$\Delta T_r = -\frac{2\sigma T_{\mathrm{m}} V_{\mathrm{s}}\, k}{\Delta H_{\mathrm{m}}} \tag{3}$$

where $\sigma$ is the solid-liquid interfacial tension, $T_{\mathrm{m}}$ is the melting point when the solid/liquid interface is a plane, $V_{\mathrm{s}}$ is the molar volume of the solid phase, $k$ is the curvature of the solid-liquid interface, and $\Delta H_{\mathrm{m}}$ is the molar enthalpy of liquid-solid transformation. According to Eq. (3), if the curvature is positive: the greater the curvature, the lower the melting point. Therefore, the edges and corners of solid particles will lead to a decrease in their equilibrium melting point, and have a priority to melt during the SSIT process, which causes the partial melting of the solid particles and makes the solid particles finer and rounder. Finally, solid particles with irregular shapes evolve to spherical or near-spherical shapes. As can be seen from Figs. 3(e), (f), and Fig. 4, the size and shape factors of solid particles in the semi-solid microstructure of the alloy increase when the isothermal temperature increases to 615 °C and 625 °C. This coarsening phenomenon of solid particles can be described by coalescence and Ostwald ripening mechanisms. The phenomenon of Ostwald ripening is the dissolution of small solid particles and the transformation of large solid particles into larger ones. Coalescence of clustered particles is the merger of adjacent particles, which leads to coarsening of solid particles through the merger of grain boundary migration. The driving force for solid particles coarsening by Ostwald ripening and coalescence of clustered particles is the reduction of interfacial free energy [24].

### 3.3.2 Effect of holding time on semi-solid microstructure

According to the analyses above, the alloy has an ideal semi-solid microstructure at 605 °C. Figure 5 shows the semi-solid microstructure of the Mg-7Zn-0.3La alloy treated at 605 °C for various times from 5 to 50 min. Figure 6 demonstrates the particle size, solid fraction, and shape factor of semi-solid Mg-7Zn-0.3La alloy held at 605 °C for different times. As shown in Fig. 5(a), a small amount of liquid phase diffuses both on boundaries and inside of the particles, and the primary solid particles do not separate significantly. After 10 min holding [Fig. 5(b)], the thickness of liquid films increases gradually. When the holding time is prolonged to 20 min, the separation of solid particles is obvious, as shown in Fig. 5(c). As observed from Fig. 5(d) and Fig. 6, when the holding time is 30 min, the size and shape factor of solid particles of the alloy are the smallest. Further extending the holding time to 40 min leads to the coarsening of the solid particles [Fig. 5(e) and Fig. 6]. When the holding time reaches 50 min, it can be seen from Fig. 5(f) that many fine solid particles are distributed around the coarse solid particles. At the same time, the coarsening, as well as coalescence of clustered particles could be still observed. The coarsening of the solid particles caused by such a long holding time is also due to the coalescence and Ostwald ripening of the solid particles to reduce the interface energy.

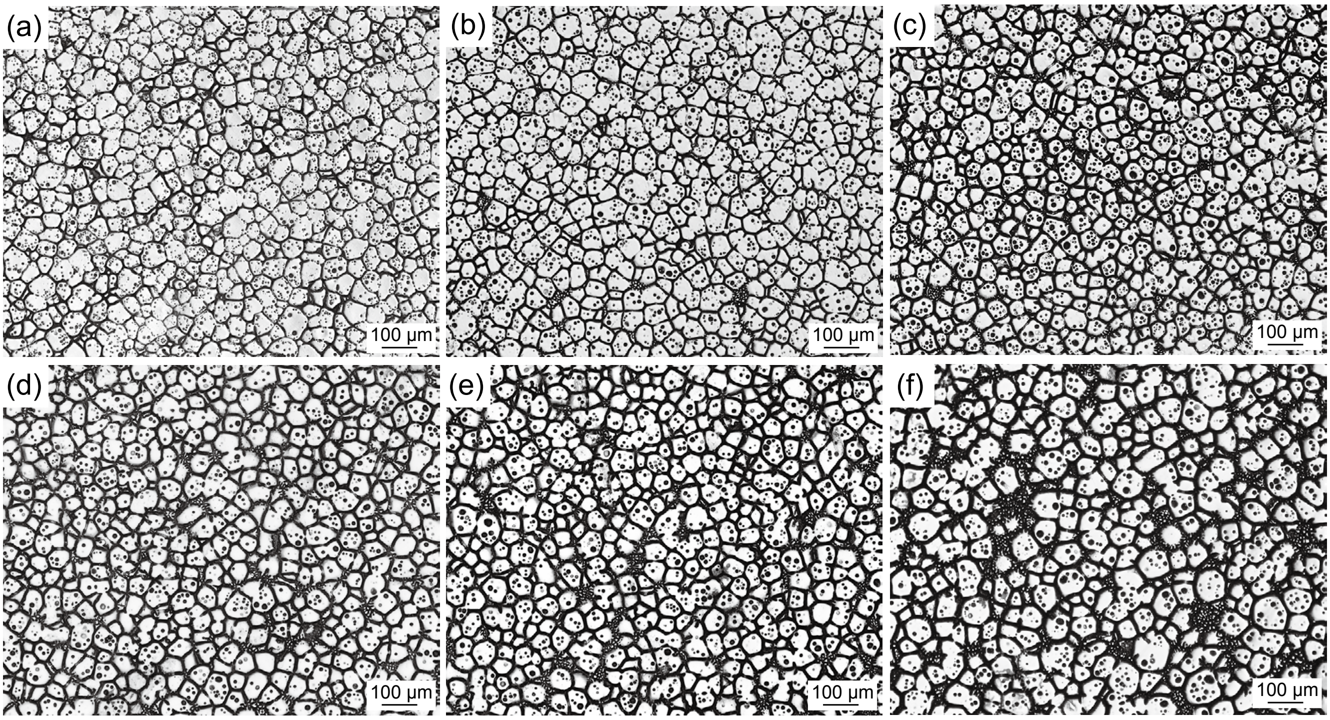


Fig. 5: Optical micrographs of semi-solid Mg-7Zn-0.3La alloy treated at 605 °C for different holding times: (a) 5 min; (b) 10 min; (c) 20 min; (d) 30 min; (e) 40 min; (f) 50 min

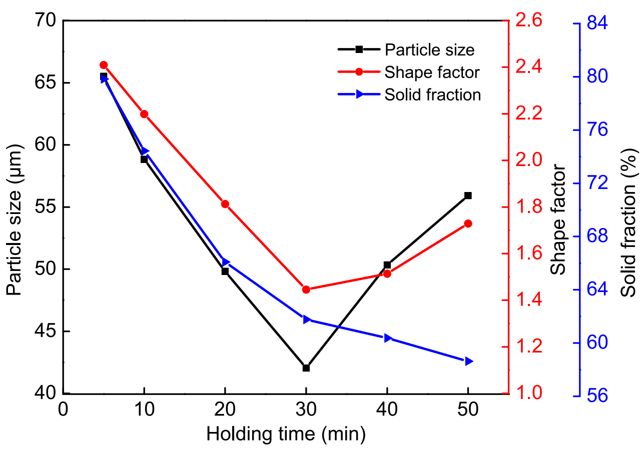


Fig. 6: Average particle size, shape factor, and solid fraction of Mg-7Zn-0.3La alloy treated at at 605 °C for different holding times

In summary, the semi-solid microstructure of Mg-7Zn-0.3La alloy obtained by holding at 605 °C for 30 min is better, and under this condition, the average solid particles' size, shape factor, and solid fraction of solid particles are 42 μm, 1.45 and 61.8%, respectively.

### 3.3.3 Semi-solid microstructural characterization

The SEM graphs of non-dendritic microstructures of the semi-solid Mg-7Zn-0.3La alloy after heat treatment at 605 °C for 30 min are shown in Fig. 7. The semi-solid microstructure of the alloy is composed of the primary solid particles (named $\alpha_1$-Mg) and liquid phase. It can be observed that the liquid phase of the semi-solid Mg-7Zn-0.3La alloy has three forms: the molten pool, the liquid pool, and the liquid film [as shown in Fig. 7(a)]. A liquid pool is formed when the liquid phase is isolated inside the solid particles. Meanwhile, the liquid phase outside the solid particles is distributed around the solid particles in the form of the molten pool and liquid film.

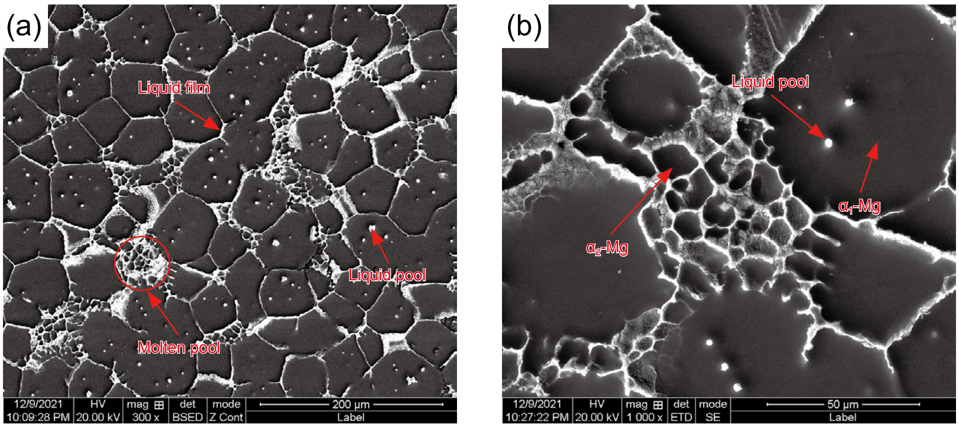


**Fig. 7: SEM images of Mg-7Zn-0.3La alloy treated at 605 °C for 30 min: (a) low magnification; (b) high magnification**

During water quenching, the liquid phase rapidly solidifies to form the secondary solidification structure, and a large number of fine eutectic grains (named $\alpha_2$-Mg) are formed during the solidification of the molten pool [as shown in Fig. 7(b)].

## 3.4 Semi-solid microstructure evolution mechanism

During the process of SSIT, the semi-solid microstructure of alloys is affected by both the melting mechanism and coarsening mechanism [27]. It can be found from Fig. 6 that with the increase of isothermal time, the coarsening of solid particles and the reduction of solid fraction occur simultaneously. This indicates that the melting and the coarsening mechanisms are not independent but work together. Therefore, it is necessary to study the coarsening process and partial melting process of solid particles.

### 3.4.1 Coarsening mechanism of solid particles

Through the research on the evolution of semi-solid microstructure in Section 3.3, it can be found that when the isothermal temperature is too high or the holding time is too long, the solid particles will be coarsened (Fig. 4 and Fig. 6). Previous research found that the coarsening of solid particles will degrade the mechanical properties of SSM processing workpieces [9, 28]. The reduction of mechanical properties caused by solid particle coarsening can be explained by the Hall-Petch relationship [9]:

$$\sigma_y = \sigma_0 + K_y d^{-\frac{1}{2}} \quad (4)$$

where $\sigma_y$ is the yield strength, $\sigma_0$ is the friction stress when dislocations glide on the slip plane, $K_y$ is the stress concentration factor constant, and $d$ is the average grain size. According to Eq. (4), the coarser the solid particle, the smaller the $\sigma_y$. Therefore, it is hoped that the coarsening rate of solid particles is low enough to prevent excessive coarsening. To investigate the coarsening of solid particles during the SSIT process, a long holding time is usually needed. Thus, the effect of La addition on the coarsening rate of solid particles during the SSIT process was examined by holding Mg-7Zn and Mg-7Zn-0.3La alloys at 605 °C for 60, 90, and 120 min, respectively. Their semi-solid structures are shown in Fig. 8. Comparing the semi-solid microstructures of Mg-7Zn and Mg-7Zn-0.3La alloys, it can be found that with the extension of holding time, the coarsening of solid particles in Mg-7Zn alloy is very significant. After holding for 120 min, the solid particles of Mg-7Zn alloy are very coarse, and the fine solid particles basically disappear [Fig. 8(c)]. Correspondingly, after holding for 120 min, a small amount of coarse solid particles appear in the semi-solid microstructure of Mg-7Zn-0.3La alloy, and there are still a large number of fine solid particles [Fig. 8(f)]. As can be seen from Fig. 8, Ostwald ripening makes a major contribution to the coarsening of solid particles, and coalescence of clustered particles could still be observed. The time dependency of the growing particle size during SSIT could be described by the Lifshitz-Slyozov-Wagner (LSW) theory [29]:

$$D_t^3 - D_0^3 = Kt \quad (5)$$

where $D_t$ is the average particle size at time $t$, $D_0$ is the average particle size of the initial solid particles, $K$ is the coarsening rate constant ($\mu m^3 \cdot s^{-1}$). Statistical analysis and linear regressions are shown in Fig. 9 to evaluate the coarsening rate constants of Mg-7Zn and Mg-7Zn-0.3La alloys during SSIT. It can be seen that the experimental data are well fitted to the LSW equation (Fig. 9). The coarsening rate constant of the alloy can be obtained from the slope of the correlating straight line. It is shown that the coarsening rate constant decreases significantly from 115.5 $\mu m^3 \cdot s^{-1}$ to 64.6 $\mu m^3 \cdot s^{-1}$ by adding 0.3% La to the Mg-7Zn alloy. The possible reason is that RE elements are surface-active elements, which can reduce the solid-liquid interfacial energy [17, 30].

### 3.4.2 Partial melting mechanism of solid particles

During the SSIT process, the partial melting mechanism plays an essential role in the evolution of semi-solid microstructure. The variation of solid fraction in semi-solid microstructure can directly reflect the partial melting of solid particles. The solid fraction decreases with the partial melting of solid particles; and also, there is no doubt that the solid fraction decreases with increasing isothermal temperature, as shown in Fig. 4. Compared with the variation of the solid fraction caused by

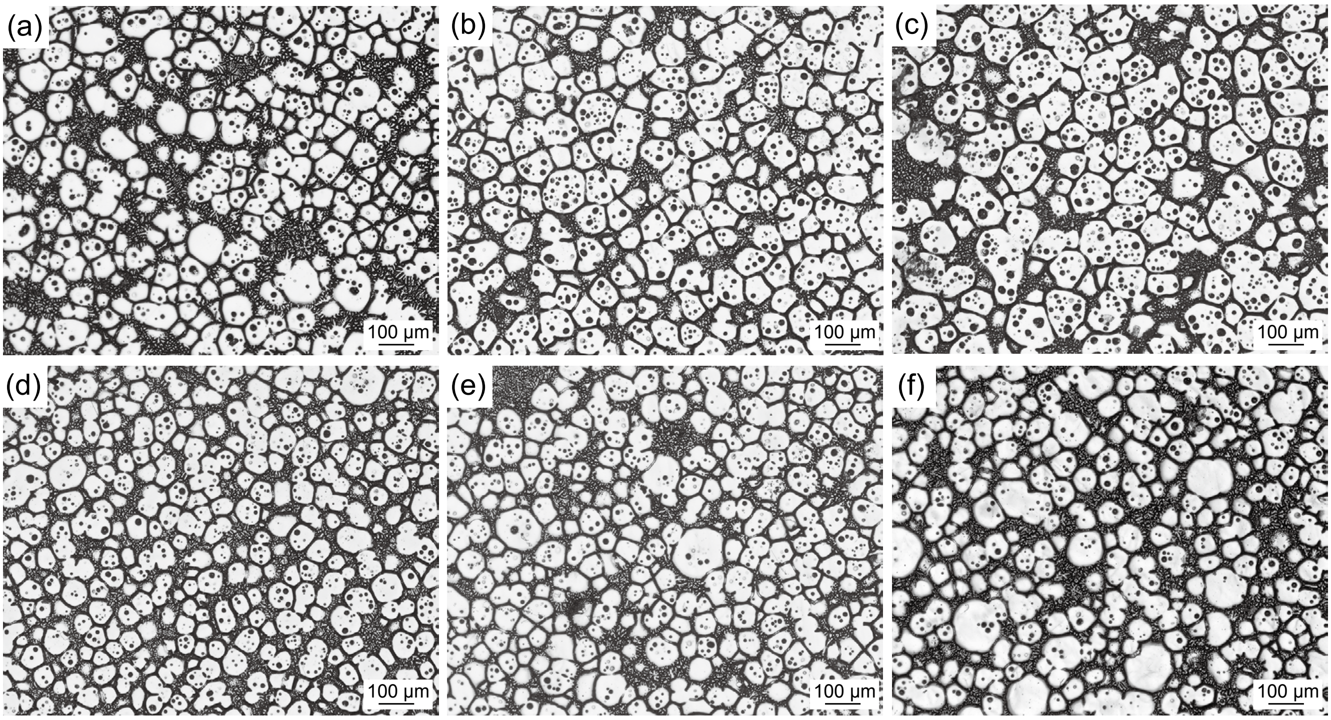


**Fig. 8: Semi-solid microstructures of Mg-7Zn (a, b, c) and Mg-7Zn-0.3La (d, e, f) alloys treated at 605 °C for 60 min (a, d), 90 min (b, e), and 120 min (c, f)**

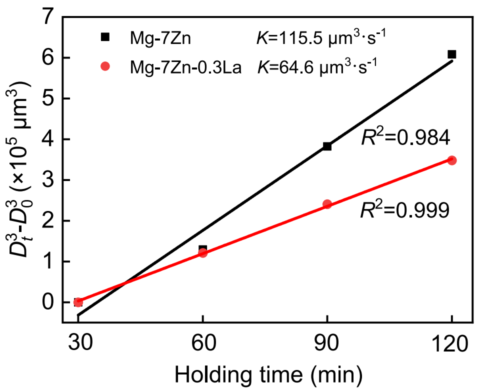


**Fig. 9: Linear fitting of primary particle coarsening of Mg-7Zn and Mg-7Zn-0.3La alloys isothermally treated at 605 °C for different times**

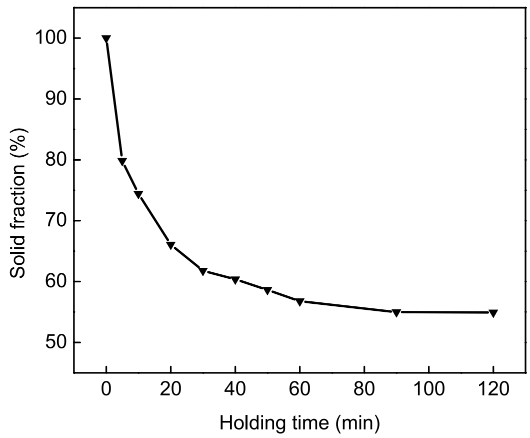


**Fig. 10: Variation of solid fraction with holding time for semi-solid Mg-7Zn-0.3La alloy at 605 °C**

variation of isothermal temperature, it is necessary to study the change of the solid fraction with increasing holding time. The variation of the solid fraction of semi-solid Mg-7Zn-0.3La alloy with holding time at 605 °C is shown in Fig. 10. It can be seen that the solid fraction decreases significantly when the holding time increases from 0 to 60 min. This indicates that solid particles partially melt during this holding time. During the SSIT process, as Zn and La atoms in the liquid phase diffuse into the solid phase, the concentration of Zn and La atoms at the edge of solid particles increases, which causes the melting point decreases. The edge part of solid particles melts into the liquid phase, which increases the content of Mg in the liquid phase. Accordingly, the concentration of Zn and La atoms decreases. When the holding time exceeds 60 min, the solid fraction of the alloy does not change obviously (Fig. 10), while the semi-solid structure has an obvious change (Fig. 8). This indicates that the melting of solid particles caused by the diffusion of Zn and La atoms becomes difficult after the holding time exceeds 60 min.

# 4 Conclusions

(1) The addition of La element can effectively refine the grain of the Mg-7Zn alloy and promote the formation of the continuous second phase, which is conducive to the separation of α-Mg during the semi-solid isothermal heat treatment (SSIT) process, resulting in a significant decrease in the particle size.

(2) Isothermal temperature and holding time play a crucial role in the average size and roundness of solid particles. The suitable processing parameter for the Mg-7Zn-0.3La alloy in SSIT is holding at 605 °C for 30 min, by which the average

solid particle size, shape factor, and solid fraction of the alloy are 42 μm, 1.45, and 61.8%, respectively.

(3) The coarsening rate constants of the semi-solid Mg-7Zn and Mg-7Zn-0.3La alloys heat treated at 605 °C are 115.5 $\mu m^3 \cdot s^{-1}$ and 64.6 $\mu m^3 \cdot s^{-1}$, respectively. Compared with the alloy without La, the coarsening rate constant of solid particles of the alloy with La addition decreases significantly.

(4) At the same isothermal heat treatment temperature, the solid fraction decreases with the increase of holding time at first, but when the solid fraction decreases to a certain degree, it no longer decreases significantly with further increase of holding time.

## Acknowledgement

This work was financially supported by the National Natural Science Foundation of China (Grant No. 51464032).

## References

[1] You Z Y, Jiang A X, Duan Z Z, et al. Effect of heat treatment on microstructure and properties of semi-solid squeeze casting AZ91D. China Foundry, 2020, 17(3): 219–226.
[2] Chen L W, Zhao Y H, Hou H, et al. Development of AZ91D magnesium alloy-graphene nanoplatelets composites using thixomolding process. Journal of Alloys and Compounds, 2019, 778: 359–374.
[3] Chen L W, Zhao Y H, Li M X, et al. Reinforced AZ91D magnesium alloy with thixomolding process facilitated dispersion of graphene nanoplatelets and enhanced interfacial interactions. Materials Science and Engineering: A, 2021, doi: 10.1016/j.msea.2021.140793.
[4] Yang M B, Pan F S, Chen R J, et al. Effects of holding temperature and time on semi-solid isothermal heat-treated microstructure of ZA84 magnesium alloy. Transactions of Nonferrous Metals Society of China, 2008, 18(3): 566–572.
[5] Atkinson H V. Semisolid processing of metallic materials. Materials Science and Technology, 2010, 26(12): 1401–1413.
[6] Luo S J, Jiang Y Z, Kang Y L. Theory and application research development of semi-solid forming in China. Transactions of Nonferrous Metals Society of China, 2010, 20(9): 1805–1814.
[7] Ranjan R, Surekha B, Ghose P. Effect of cooling slope process parameters on non-dendritic feedstock production: A comprehensive review. Journal of the Institution of Engineers (India): Series C, 2021, 102: 821–842.
[8] Huang X F, Ma Y J, Zhang Q Q, et al. Effects of trace Cr on as-cast microstructure and microstructural evolution of semi-solid isothermal heat treatment ZC61 magnesium alloy. China Foundry, 2019, 16(1): 53–62.
[9] Wang L P, Chen T, Jiang W Y, et al. Grain coarsening in semi-solid state and tensile mechanical properties of thixoformed AZ91D-RE. Journal of Rare Earths, 2013, 31(3): 319–326.
[10] Xin T Z, Zhao Y H, Mahjoub R, et al. Ultrahigh specific strength in a magnesium alloy strengthened by spinodal decomposition. Science Advances, 2021, 7(23): eabf3039.
[11] Wu G H, Wang C L, Sun M, et al. Recent developments and applications on high-performance cast magnesium rare-earth alloys. Journal of Magnesium and Alloys, 2021, 9(1): 1–20.
[12] Hu Y, Rao L, Ni X W. Effect of isothermal heat treatment on semi-solid microstructure of AZ91D magnesium alloy containing rare earth Gd. China Foundry, 2015, 12(1): 20–25.
[13] Xie J S, Zhang J H, You Z H, et al. Towards developing Mg alloys with simultaneously improved strength and corrosion resistance via RE alloying. Journal of Magnesium and Alloys, 2021, 9(1): 41–56.
[14] Seyed M A and Reza M. Effects of Gd, Y, and La rare-earth elements on the microstructural stability and elevated-temperature mechanical properties of AZ81 magnesium alloy. Metallurgical and Materials Transactions A, 2019, 50(12): 5957–5968.
[15] Zhang J L, Feng Z Y, Hu L Q, et al. Precipitation behavior of AZ91 magnesium alloys with different La contents. Acta Metallurgica Sinica, 2012, 48(5): 607–614. (In Chinese)
[16] Du Y Z, Zheng M Y, Qiao X G, et al. Effect of La addition on the microstructure and mechanical properties of Mg-6wt.%Zn alloys. Materials Science and Engineering A, 2016, 673: 47–54.
[17] Nami B, Shabestari S G, Miresmaeili S M, et al. The effect of rare earth elements on the kinetics of the isothermal coarsening of the globular solid phase in semisolid AZ91 alloy produced via SIMA process. Journal of Alloys and Compounds, 2009, 489(2): 570–575.
[18] Rogal L. Critical assessment: Opportunities in developing semi-solid processing: Aluminium, magnesium, and high-temperature alloys. Materials Science and Technology, 2017, 33(7): 759–764.
[19] Hiroaki O. Supplemental literature review of binary phase diagrams: Cs-In, Cs-K, Cs-Rb, Eu-In, Ho-Mn, K-Rb, Li-Mg, Mg-Nd, Mg-Zn, Mn-Sm, O-Sb, and Si-Sr. Journal of Phase Equilibria and Diffusion, 2013, 34(3): 251–263.
[20] Chen X Q, Liu J W, Luo C P. Research status and development trend of Mg-Zn alloys with high strength. Materials Reports, 2008, 22(5): 58–62.
[21] Qin M L. The influence of thermal treatment on Mg-xZn alloy and semi-solid water quenching microstructure. Master's Dissertation, Lanzhou: Lanzhou University of Technology, 2016: 56–60.
[22] Buha J. Reduced temperature (22–100 °C) ageing of an Mg-Zn alloy. Materials Science and Engineering A, 2008, 492: 11–19.
[23] Ren Y P, Liu B S, Xie H B, et al. Characterization of precipitates in aged Mg-4wt.%Zn alloy. Materials Today Communications, 2021, 26: 102017.
[24] Fan Z. Semisolid metal processing. International Materials Reviews, 2002, 47(2): 49–85.
[25] Fu L, Wang X B, Gou P L, et al. Microstructures and tensile properties of AZ91 magnesium alloys with Ca, Sm, and La elements additions. Advanced Engineering Materials, 2017, 19(12): 1700230.
[26] Feng K, Huang X F, Ma Y, et al. Microstructure evolution of ZA72 magnesium alloy during partial remelting. China Foundry, 2013, 10(2): 74–80.
[27] Fan L L, Zhou M Y, Zhang Y W X, et al. The semi-solid microstructural evolution and coarsening kinetics of AZ80-0.2Y-0.15Ca magnesium alloy. Materials Characterization, 2019, 154: 116–126.
[28] Zhao Z D, Chen Q, Kang F, et al. Microstructural evolution and tensile mechanical properties of thixoformed AZ91D magnesium alloy with the addition of yttrium. Journal of Alloys and Compounds, 2009, 482(1): 455–467.
[29] Loué W R and Suéry M. Microstructural evolution during partial remelting of Al-Si7Mg alloys. Materials Science and Engineering A, 1995, 203(1): 1–13.
[30] Tang Q, Sun H, Zhou M Y, et al. Effect of Y addition on the semi-solid microstructure evolution and the coarsening kinetics of SIMA AZ80 magnesium alloy. Metals, 2017, 7(10): 416.